URSI GASS 2020, Rome, Italy, 29 August - 5 September 2020

Compact Dual-Polarized Metasurface Antenna with Extended Axial Ratio Beamwidth for S and C-band Applications

Mohammad Ameen*(1), and Raghvendra Kumar Chaudhary(2)
(1),(2)Department of Electronics Engineering, Indian Institute of Technology (Indian School of Mines), Dhanbad, India
(1)mohammadmn61@gmail.com, and (2)raghvendra.chaudhary@gmail.com

Abstract

This work discusses the design of a triple-band and dual-polarized high gain circularly polarized (CP) antenna based on artificial transmission line (ATL) based metamaterial (MTM) structures. To enhance the gain and extend the axial ratio (AR) beamwidth, a new multi-band artificial magnetic conductor (AMC) based metasurface (MS) is placed below the radiating triple-band antenna. Due to this, the impedance bandwidth (IBW), gain and AR beamwidth is enhanced. The intended antenna provides overall dimensions of 0.36 $\lambda_0 \times 0.36\ \lambda_0 \times 0.10\ \lambda_0$ at 2.57 GHz. Also, the antenna is capable of providing positive gain value and extended AR beamwidth for theta = $\pm 58^0$ and phi = 0^0 to 360^0 at 2.45 GHz. Hence the intended antenna is suitable for working in small satellite applications at S and C bands.

1 Introduction

The recent antenna systems for military and satellite application systems are pointing towards miniaturization with enhanced performance [1]. For this purpose, ATL antennas based on composite right/left-handed (CRLH) transmission line (TL) structures are the best candidature for miniaturization. The ATL antennas provide left-handed (LH) properties which are not noticeable in right-handed (RH) antennas [1]. These antennas can be realized using CRLH [1], epsilon-negative [2] and mu-negative TLs [3] for miniaturization purposes. Various number of CP antennas using ATL are depicted in [1]–[3]. Unfortunately, these antennas provide narrow IBW, narrow ARBW and negative gain, and lesser radiation efficiency with higher design complexity by implementing complex vias [2].

To enhance the performance of ATL based antennas explained above, the use of MS-based structures combined with radiator antenna and enhance the antenna radiation performance in terms of gain, IBW, and efficiency. Several antenna configurations utilizing MS are explained in [4]–[7]. These reported antenna sizes are quite large, and it is very difficult to accommodate with newer systems. In this work, a multilayer dual-polarized and tri-band antenna with higher gain and enhanced IBW compared with the antennas in [4]–[7] are explained in Table 1. The MS antenna first band at 2.45 GHz can provide a positive gain and extended AR beamwidth for theta = $\pm 58^0$ and phi = 0^0 to 360^0. Hence the intended antenna is applicable for small satellite and military applications in S and C-bands.

Table. 1. Comparison of the intended MS loaded antenna with existing MS antennas

Ref. No.	Freq. (GHz)	Total antenna size (mm^3)	IBW (%)	AR (%)	Via
[4]	4.0	39.3 × 45.7 × 5.5	16	10	No
[5]	2.50	35 × 35 × 3.7	5.2	1.6	Yes
[6]	2.86	43.5 × 43.5 × 12.4	1.05	1.05	Yes
	3.11		1.61	1.61	
[7]	1.33	70 × 70 × 2	1.88	–	Yes
	1.88		3.24	–	
	2.412		10.03	1.0	
This work	2.57	42.5 × 42.5 × 12.8	9.33	2.43	No
	3.16		8.86	–	
	4.51		38.13	4.39	

2 Proposed Antenna Geometry and Design

2.1 Design of ATL based LP Antenna

The schematic view of the ATL loaded antenna is depicted in Figure 1(a). The antenna consists of asymmetric co-planar ground (ACPG) with an inverted '*L*' shaped feed line. The antenna is designed on FR-4 substrate with thickness H_1 = 1.6 mm, ε_r = 4.4, and tanδ = 0.02. The simulated input reflection coefficient (S_{11}) and gain of the LP antenna is plotted in Figure 1(b). The equivalent circuit model of the LP antenna is shown in Figure 2. The antenna feed line provides series inductance (L_1). The coupling between the feed line and ACPG supports capacitance (C_1). The semicircle of radius R_1 and rectangular strip ($W_f \times L_6$) provides series inductances (L_{R1} and L_{R2}). The gap g_2 introduces series capacitance (C_L). The shunt inductance (L_L) is provided by a thin strip of dimension $W_3 \times L_3$, which is terminated by a rectangular stub of $W_2 \times L_2$ for providing the virtual ground. The shunt capacitor (C_R) is provided by the coupling between semi-circle, rectangular stub, and the ACPG. The antenna provides an IBW of 20.74% (2.64–3.25 GHz) and a gain of 2.50 dBi at 2.94 GHz. The optimized dimensions are L = 38, L_1 = 12, L_2 = 5, L_3 = 9.02, L_4 = 5, L_5 = 18, L_6 = 10, W_L = 20.7, W_f = 3, W_1 = 2, W_2 = 8, W_3 = 0.9, $g_1 = g_2$ = 0.3, and R_1 = 5 (All dimensions are in mm). Figure 3(a) and 3(b) depicts the parametric study on varying the series and shunt elements of ATL and it is noted that there is no significant variation in series parameters (R_1 and g_2) and more significant variation in shunt parameters (L_3 and W_3). Hence, the antenna depicted in Figure 1(a) depends on the open-ended boundary conditions [1]. The resonance frequency is managed by varying the shunt arm (L_L, C_R, and C_S) of the CRLH-TL.

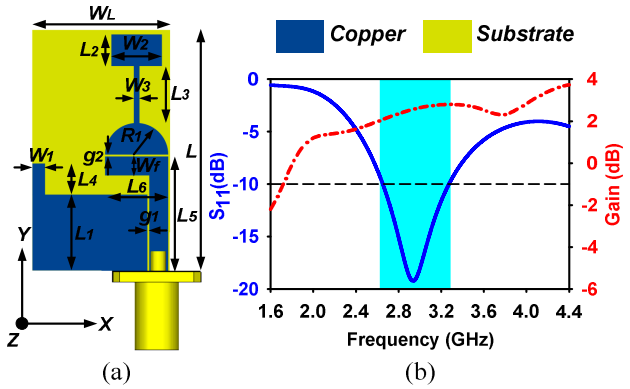

Figure 1. CRLH-TL LP antenna. (a) Antenna geometry, (b) Input reflection coefficient (S_{11}), and gain response.

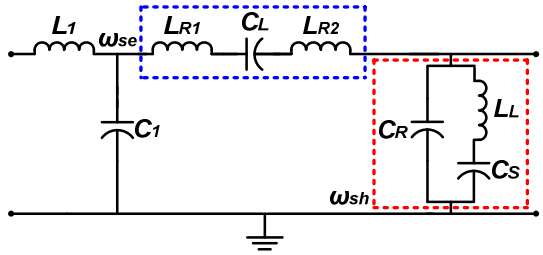

Figure 2. Approximate equivalent circuit model of the intended ATL loaded LP antenna.

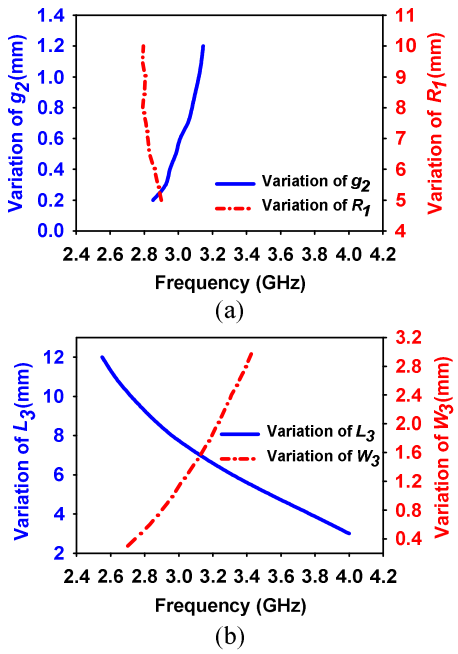

Figure 3. LP antenna results. (a) Variation of series parameters and (b) Variation of shunt parameters.

2.2 Design of ATL based CP Antenna

The schematic view of the ATL based CP antenna is depicted in Figure 4(a). The antenna design is similar to the case of LP antenna in section 2.1 except an additional rectangular strip ($W_3 \times L_7$) is introduced. For generating CP radiation and extending IBW, the same ATL unit cell used in the LP antenna is placed orthogonally as shown in Figure 4(a). The two ATL unit cells will generate degenerate mode

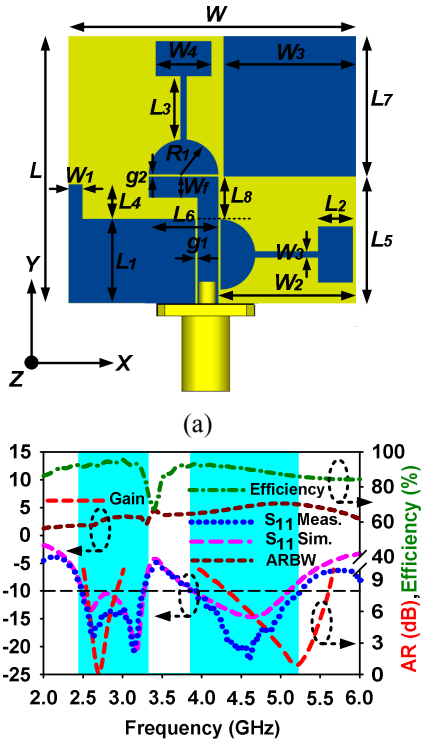

Figure 4. CRLH-TL CP antenna. (a) Antenna geometry, (b) Antenna parameters.

which results in CP radiation. The S_{11} plot in Figure 4(b) reveals that the antenna provides two wider band ranges from (2.45–3.32 GHz) 30.15% and (3.86–5.14 GHz) 28.44% with an inband ARBW of (2.54–2.94 GHz) and (4.30–5.14 GHz). The CP antenna provides a gain of 3.2 dBi and 5.4 dBi at 2.88 GHz and 4.50 GHz. Also, the radiation efficiency is better than 88% for the two bands. From Figure 5(a) and 5(b), the better CP radiation and good IBW is obtained by varying the dimension L_8 and better

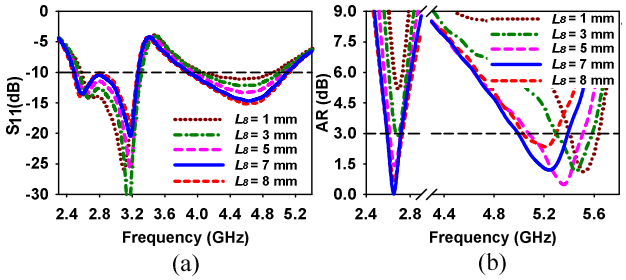

Figure 5. Antenna results by varying L_8. (a) S_{11} and (b) AR.

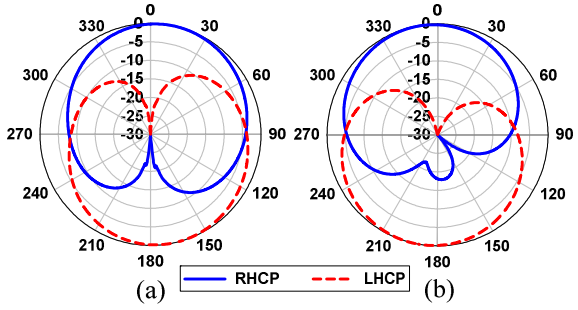

Figure 6. Simulated 2D radiation pattern of CP radiator antenna at 2.74 GHz. (a) *xz*-plane, and (b) *yz*-plane.

results are obtained at L_8 = 7 mm. The originality of the antenna design is very simple and easy to control CP radiation and the use of ACPG can achieve wider IBW. The complete size of the ATL based CP antenna is 0.38 λ_0 × 0.36 λ_0 × 0.015 λ_0 at 2.88 GHz. The radiation pattern depicted in Figure 6 identifies that the antenna offers RH-CP radiation in +*Z* direction and LH-CP radiation in -*Z* direction for the two principal planes at 2.74 GHz.

3 Design and Analysis of AMC-MS

The AMC-MS can enhance the radiator antenna IBW and gain [2]. Figure 7(a) interprets the AMC-MS configuration inspired by the previous work [8]. The reflection phase response is plotted in Figure 7(b). The MS is designed on FR-4 substrate with thickness H_3 = 3.2 mm, ε_r = 4.4, and $tan\delta$ = 0.02. The MS consists of side-blended square-shaped ring and Jerusalem cross structure. The reflection response in Figure 7(b) shows ±90° reflection phase from 2.34–2.57 GHz and this range can be work as AMC and 4.18–4.95 GHz frequency range will work as perfect electric conductor. The optimized AMC-MS dimensions are L_a = L_b = 42.5, a = b = 10.63, c = 5.5, d = 1, e = f = 2.375, g = 0.75, h = 3.5, and I = 0.5 (All units are in mm).

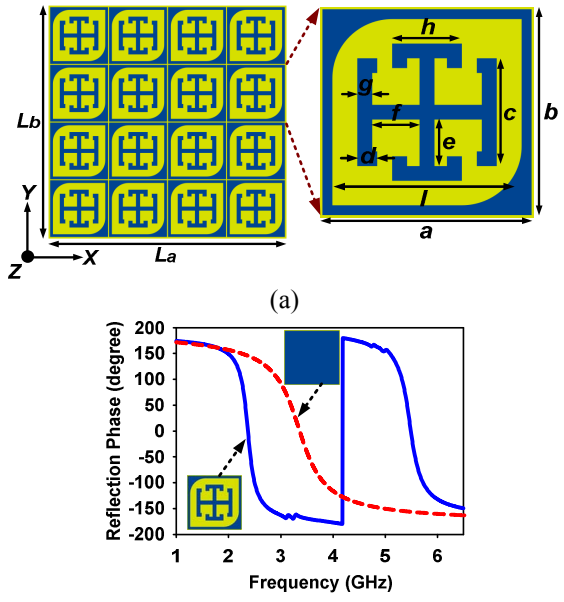

(a)

(b)

Figure 7. MS design results. (a) schematic overview of the MS, and (b) reflection phase responses.

4 ATL loaded Antenna over AMC-MS

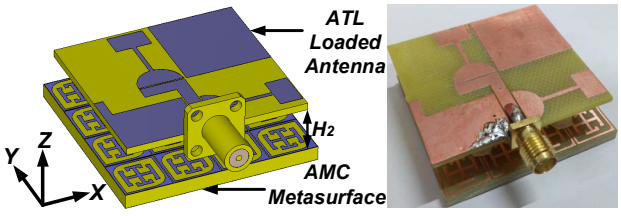

(a) (b)

Figure 8. Final MS loaded antenna. (a) 3D schematic model, (b) Photograph of fabricated antenna.

The final three-layer MS antenna is depicted in Figure 8. The top layer is a dual-band CP antenna designed in section 2.2 and the middle is air layer of height H_2 = 8 mm. Below that, AMC-MS designed in section 3 is placed. Figure 9(a)–(c) shows the study on the spacing between the radiator and MS-based on S_{11}, AR and gain responses from H_2 = 4mm to 20 mm. It is noted that increasing H_2, the first wider band splits into two bands and the S_{11} response of the third band centered at 4.34 GHz degrade and better AR obtained at H_2 = 8 mm. Hence by considering the antenna profile, IBW, gain, and AR, the optimized value of H_2 = 8 mm is fixed. Figure 10(a) and 10(b) plots the AR and gain response for various theta and phi values. It is noticed that a positive gain values and AR< 3 dB is obtained for theta = ±58^0 and phi = 0^0 to 360^0 is obtained at 2.45 GHz suitable for small satellite application systems.

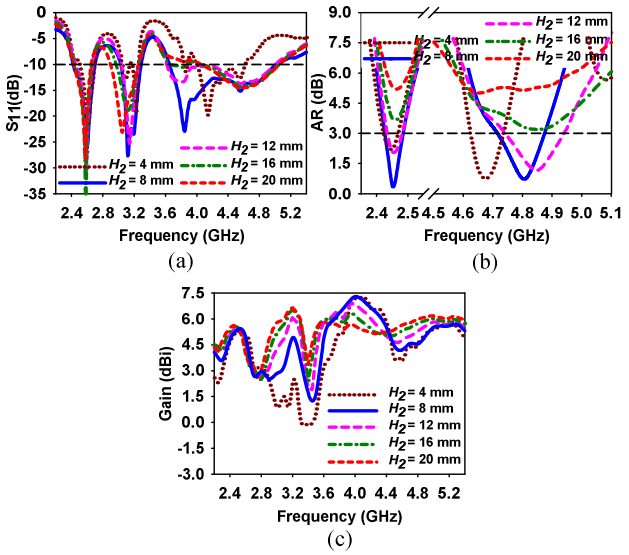

(a) (b)

(c)

Figure 9. MS loaded antenna results by varying H_2. (a) variation of S_{11}, (b) variation of the AR, (c) variation of gain

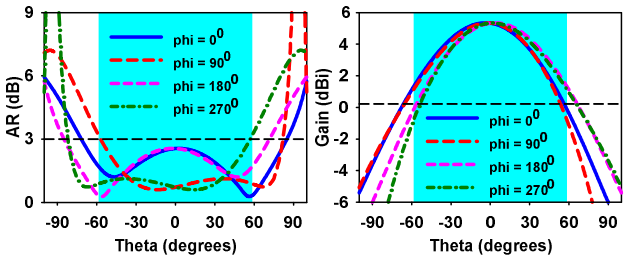

(a) (b)

Figure 10. Simulated antenna results for theta = ±58^0 and phi = 0^0 to 360^0. (a) AR response, and (b) gain response

5 Results and Discussions

The 10-dB BW for the MS antenna ranges from 2.46–2.70 GHz, 3.02–3.30 GHz, and 3.65–5.37 GHz with a percentage bandwidths of 9.33%, 8.86%, and 38.13% respectively as depicted in the Figure. 11(a). The ARBW is 2.43–2.49 GHz and 4.68–4.89 GHz as depicted in Figure 11(b). A maximum gain of 5.38 dBi, 4.92 dBi, and7.29 dBi, is obtained at 2.47 GHz, 3.20 GHz and 4.0 GHz as depicted in Figure 11(c). The radiation efficiency of 77.5%, 68.5%, and 88.6% is obtained for the three successive bands depicted in Figure 11(d). The 2D radiation patterns of the

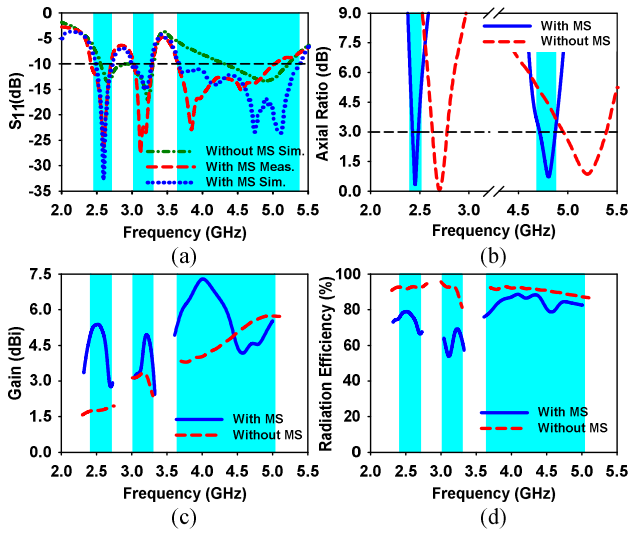

Figure 11. Antenna results with and without MS. (a) S_{11}, (b) simulated AR, (c) gain, and (d) efficiency.

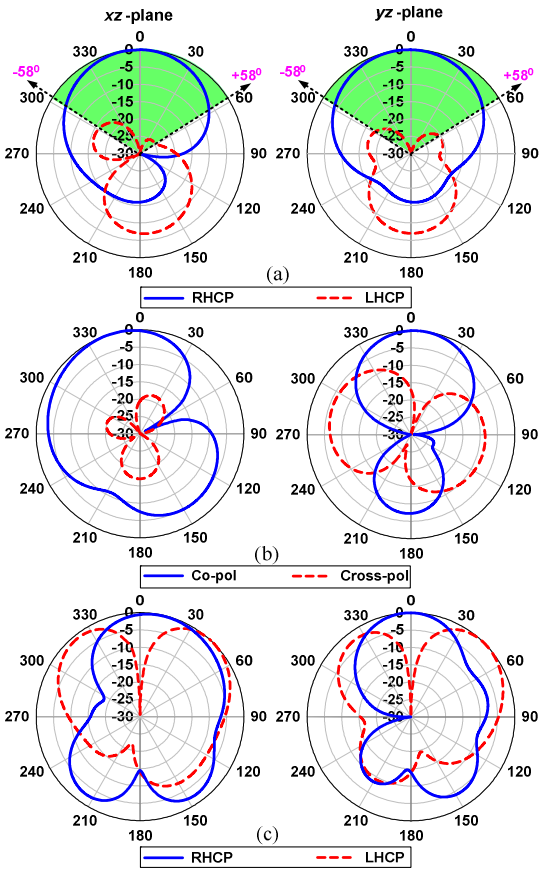

Fig. 12. Simulated 2D radiation patterns of the antenna with MS. (a) 2.45 GHz, (b) 3.22 GHz and (c) 4.80 GHz.

MS loaded antenna are plotted in Figure 12(a)–12(c) at 2.45 GHz, 3.22 GHz, and 4.8 GHz respectively. From the radiation patterns, it can be seen that for the first band (2.45 GHz) and third band (4.8 GHz) provides RHCP radiation in the broadside direction. The second band at 3.22 GHz provides LP radiation in the broadside radiation. Here a slight tilt is noticed at 3.22 GHz and 4.80 GHz due to the non-symmetric antenna geometry of the radiator.

6 Conclusion

This paper exploits a new idea to generate multilayer triple-band and dual-polarized antenna with extended AR beamwidth for small satellite and military applications. The CP characteristics are obtained due to the placement of similar CRLH TL based unit elements in an orthogonal manner. The antenna provides a smaller size of 0.36 λ_0 × 0.36 λ_0 ×0.10 λ_0 at 2.56 GHz due to ATL property.

7 Acknowledgements

This research work is supported by Science and Engineering Research Board (SERB), DST, Government of India under grant number EEQ/2016/000023.

8 References

1. M. Ameen and R. K. Chaudhary, "Metamaterial-based Wideband Circularly Polarised Antenna with Rotated V-shaped Metasurface for Small Satellite Applications," *Electron. Lett.*, **55**, 7, April 2019, pp. 365–366, doi: 10.1049/el.2018.7348

2. M. Ameen and R. K. Chaudhary, "Metamaterial Circularly Polarized Antennas: Integrating an Epsilon Negative Transmission Line and Single Split Ring-type Resonator," *IEEE Antennas Propag. Mag.*, January 2020, doi: 10.1109/ MAP.2019.2950920

3. B. Park and J. Lee, "Compact Circularly Polarized Antenna With Wide 3-dB Axial-Ratio Beamwidth," *IEEE Antennas Wireless Propag. Lett.*, **15**, June 2016, pp. 410–413, doi: 10.1109/LAWP.2015.2448553

4. T. Yue, *et. al*, "Compact, Wideband Antennas Enabled by Interdigitated Capacitor-Loaded Metasurfaces," *IEEE Trans. Antennas Propag.*, **64**, 5, May 2016, pp. 1595–1606, doi: 10.1109/TAP.2016.2535499

5. K. Agarwal, Nasimuddin, *et. al*, "RIS-Based Compact Circularly Polarized Microstrip Antennas," *IEEE Trans. Antennas Propag.*, **61**, 2, February 2013, pp. 547–554. doi: 10.1109/TAP.2012.2225816

6. H. Xu, G. Wang, J. Liang, *et. al*, "Compact Circularly Polarized Antennas Combining Meta-Surfaces and Strong Space-Filling Meta-Resonators," *IEEE Trans. Antennas Propag.*, **61**, 7, July 2013, pp. 3442–3450, doi: 10.1109/TAP.2013.2255855

7. W. Cao, B. Zhang, A. Liu, *et. al*, "Multi-Frequency and Dual-Mode Patch Antenna Based on Electromagnetic Band-gap (EBG) Structure," *IEEE Trans. Antennas Propag.*, **60**, 12, December 2012, pp. 6007–6012. doi: 10.1109/TAP.2012.2211554

8. M. Ameen, V. R. Ramireddy and R. K. Chaudhary, "A Compact Dual-Band and Dual-Polarized Open-Ended ZOR Antenna with AMC Ground Plane for 4G-LTE/WLAN/WiMAX Applications," *IEEE Indian Conf. Antennas Propog.*, India, 2018, pp. 1–4. doi: 10.1109/INCAP.2018.8770831